Star-Shaped Donor-π-Acceptor Conjugated Oligomers with 1,3,5-Triazine Cores: Convergent Synthesis and Multifunctional Properties

Shijie Ren,[†] Danli Zeng,[†] Hongliang Zhong,[†] Yaochuan Wang,[‡] Shixiong Qian,*[,‡] and Qiang Fang*[,†]

Key Laboratory of Organofluorine Chemistry and Laboratory for Polymer Materials, Shanghai Institute of Organic Chemistry, Chinese Academy of Sciences, 345 Lingling Road, Shanghai 200032, P. R. China, and Surface Physics Lab (National Key Lab) and Physics Department, Fudan University, 220 Handan Road, Shanghai 200433, P. R. China

Received: May 22, 2010; Revised Manuscript Received: July 15, 2010

Monodispersed oligomers have been widely developed and used in different optoelectronic areas due to their well-defined molecular structures, high purity, and solution processability. Star-shaped oligomers are especially interesting for OLED application because of their antiaggregation abilities and stable electroluminescence. In addition, star-shaped donor-π-acceptor conjugated molecules are known to afford good nonlinear optical and two-photon absorption properties due to the intramolecular charge transfer and cooperative enhancement effects. In this context, three generations of highly soluble 1,3,5-triazine based donor-π-acceptor compounds, **TFT1**, **TFT2**, and **TFT3**, were prepared through a convergent synthetic strategy and their optoelectronic properties were fully studied, which showed distinct correlations with the structures. Closed-aperture and open-aperture *Z*-scan methods were employed to measure the nonlinear refractive index and two-photon absorption properties of the oligomers, respectively. **TFT1** showed a high nonlinear refractive index of 4.14×10^{-12} esu in THF solution with an excitation wavelength of 800 nm. Also, **TFT1** exhibited a large two-photon absorption cross section of 234 GM and a frequency up-converted two-photon excited fluorescence with a λ_{TPEF}^{max} value of 527 nm under 800 nm laser irradiation with a pulse duration of 140 fs. OLED devices using the spin-coated films of these oligomers as an active layer showed intensive blue electroluminescence with a maximum luminance of 3093 cd/m^2 at a current efficiency of 1.47 cd/A from **TFT1**.

Introduction

In the past two decades, extensive research attention has been paid to high-performance organic materials used in optoelectronic fields, such as organic light-emitting diodes (OLEDs),[1] organic solar cells,[2] and organic thin-film transistors.[3] At present, there are manly two kinds of materials being developed for organic electronics: small molecules[1a,4] and conjugated polymers.[5] However, both groups of material have certain drawbacks. Organic small molecules are prone to crystallization, and typically high temperature vacuum deposition has to be used to fabricate the devices. On the other hand, although they can be processed simply with methods such as spin-coating and inkjet printing, polymer materials are more difficult to purify and thus stability and reproducibility remain big problems. In recent years, monodispersed oligomers or dendrimers which sit between small molecules and polymers have gradually attracted more and more attention and become a third choice of the organic optoelectronic materials.[6] Ideally, they can combine the advantages of both conjugated polymers and small molecules together, such as good solution processability and well-defined molecular structure.

Compared with their linear counterparts, conjugated star-shaped molecules have exhibited some special merits guaranteed by the unique structures.[7] Branched molecular configuration can afford better electroluminescent stability due to less aggregation in the solid state, and the fact that more functional groups can be merged into the branched structure means there are more opportunities to fine-tune the optoelectronic performances and to study the relationship between structures and properties. Putting an electron donor and acceptor into one molecule can normally lead to broad absorption, lower band gap, easily tuned fluorescence, and good nonlinear optical properties.[8] Also, multibranched structures are known to bring cooperative enhancement in terms of conjugation expansion and two-photon absorption (TPA) properties.[9]

1,3,5-Triazine containing materials have been widely used in industry owing to their high thermal stability derived from the structural symmetry of 1,3,5-triazine units,[10] and recently quite a bit of attention has been paid to 1,3,5-triazine containing π-conjugated systems because of the unique properties such as high electron deficiency and spatial coplanarity.[11] 1,3,5-Triazine based small molecules and conjugated polymers have been employed as electron transporting and hole blocking materials,[11b,c,12] emissive layers,[13] or host materials for phosphorescent dyes[14] in OLED devices. For TPA application, a series of star-shaped 1,3,5-triazine based chromophores were reported in 2004,[15] which showed promising TPA properties because of strong intramolecular charge transfer (ICT). In that paper, the authors discussed the effects of different side chains on the properties. Recently, star-shaped novel donor-π-acceptor (D-π-A) molecules containing 1,3,5-triazine-2,4,6-trithiophene units were published and therein different donor groups and π-conjugated bridges were studied according to their influences on the TPA performance.[16]

* To whom correspondence should be addressed. E-mail: qiangfang@mail.sioc.ac.cn.
[†] Chinese Academy of Sciences.
[‡] Fudan University.

10.1021/jp104710y

However, there have only been limited reports on the use of 1,3,5-triazine based oligomers or dendrimers as organic electronic materials,[17] which are supposed to be advantageous in terms of film-forming and solution processability. Here, we report the synthesis and characterization of a series of 1,3,5-triazine cored star-shaped oligomers. The performance of the novel D-π-A dendrimers in OLEDs and their nonlinear optical properties were investigated. The results show good structure−property correlation and promising OLED device behavior and decent TPA cross sections were achieved.

Experimental Section

Reagents and Instruments. Chemical reagents and solvents were purchased from Acros or Aldrich and used without further purification unless otherwise noted. Toluene and THF were distilled from sodium, and dichloromethane and chloroform were distilled over KOH. The starting compounds 2-bromo-9,9-dioctyl-fluorene (**1**),[18] 4-bromo-*N*,*N*-diphenylaniline (**3**),[19] and 2,7-dibromo-9,9-dioctyl-fluorene (**5**)[18] were prepared according to published procedures. All air and water sensitive reactions were performed under a dry argon atmosphere.

^{1}H NMR and ^{13}C NMR spectra were recorded on a Bruker DPX 400 or Varian mercury 300 spectrometer using $CDCl_3$ as solvent and TMS as internal standard, respectively. Mass spectra were taken with a HP 5989A or Finnigan 4021 mass spectrograph. Elemental analysis was performed with an Elementer Vario EL elemental analyzer. UV−vis and PL spectra were obtained with a Hitachi UV-2910 and a Hitachi F-4500 spectrophotometer, respectively. Thermal stability was determined with a TGA Q500 thermogravimetric analyzer at a heating rate of 10 °C min^{-1} in nitrogen. Cyclic voltammetry of the cast films of the compounds on ITO glass (working electrode) was measured in an acetonitrile solution of Bu_4NBF_4 (0.10 M) under argon using (0.10 M $AgNO_3$)/Ag and platinum wire as reference and counter electrodes, respectively. The ferrocenium/ferrocene (Fc^+/Fc) couple was used as the internal standard. A CHI 600B analyzer was used for the cyclic voltammetry.

Synthesis. ***9,9-Dioctyl-9H-fluorene-2-carbonitrile (2).*** A mixture of **1** (2.192 g, 4.674 mmol) and CuCN (0.627 g, 7 mmol, 1.5 equiv) in NMP (40 mL) was purged with argon and refluxed overnight. Then, the reaction temperature was reduced to about 120 °C and 4 g of $FeCl_3$ in 2 mL of concentrated HCl and 10 mL of distilled H_2O were added into the dark solution. The mixture was stirred for a further 30 min. After being cooled at room temperature, the mixture was extracted with toluene (150 mL) twice and the organic layer was washed with 100 mL of 6 N HCl, water, 10% NaOH solution, and water again prior to being dried over Na_2SO_4. The solvent was then removed under reduced pressure to give a crude product. The crude product was purified by column chromatography using CH_2Cl_2/petroleum ether (20/80, v/v) as eluent to give **2** as a colorless viscous liquid in a yield of 68%. ^{1}H NMR (300 MHz, $CDCl_3$, δ): δ 7.73−7.78 (2H, m), 7.60−7.65 (2H, m), 7.36−7.39 (3H, m), 1.97 (4H, m), 1.04−1.22 (20H, m), 0.82 (6H, t), 0.54 (4H, m). FT-IR (NaCl pellets, cm^{-1}): 2927, 2855, 2224, 1610, 1458, 1380, 740. MS (EI), *m*/*z* 416 (M^+).

2,4,6-Tris(9,9-dioctyl-9H-fluoren-2-yl)-1,3,5-triazine (**FT1*****).*** To a vigorously stirring solution of trifluoromethanesulfonic acid (2 mL) was added dropwise **2** (1.313 g, 3.164 mmol) in dry $CHCl_3$ (3 mL) over about 10 min at 0 °C under an Ar atmosphere. After being stirred at room temperature for 2 days, the mixture was diluted with 100 mL of $CHCl_3$ and poured into 100 mL of 10% NH_4OH aqueous solution. The organic layer was separated, washed twice with water, and then dried over Na_2SO_4. The solvent was removed under reduced pressure to give a crude product, which was further purified by column chromatography using CH_2Cl_2/petroleum ether (10/80, v/v) as eluent to offer **FT1** as a transparent viscous liquid in a yield of 91%. ^{1}H NMR (300 MHz, $CDCl_3$, δ): 8.85 (3H, d), 8.76 (3H, s), 7.94 (3H, d), 7.84 (3H, m), 7.38−7.43 (9H, m), 2.12 (12H, m), 1.02−1.20 (60H, m), 0.65−0.82 (30H, m). ^{13}C NMR (100 MHz, $CDCl_3$, δ): 171.83, 151.97, 151.13, 145.55, 140.38, 135.34, 128.28, 128.04, 126.95, 123.31, 123.10, 120.52, 119.77, 55.28, 40.37, 31.80, 30.08, 29.27, 29.24, 23.86, 22.59, 14.04, 13.85. FT-IR (NaCl pellets, cm^{-1}): 2928, 2854, 1609, 1579, 1513, 1466, 1370, 823, 740. MS (MALDI-TOF): *m*/*z* 1247.1 (M^+). Anal. Calcd for $C_{90}H_{123}N_3$: C, 86.69; H, 9.94; N, 3.37. Found: C, 87.00; H, 10.14; N, 3.36.

N,N-Diphenyl-4-(4,4,5,5-tetramethyl-1,3,2-dioxaborolan-2-yl)aniline (4). 13.4 mL (21.5 mmol, 1.25 equiv) of n-BuLi (1.6 M in hexane) was added through a syringe over about 30 min to a solution of **3** (5.575 g, 17.2 mmol) in dry THF (150 mL) at −78 °C. The mixture was stirred for 1 h at the temperature, and then, 9.7 g (51.6 mmol, 3 equiv) of boronic acid triisopropylester was added. After being stirred overnight at room temperature, the reaction mixture was poured into 200 mL of water and extracted with ethyl acetate. The organic layer was washed with water three times and dried over Na_2SO_4. The solvent was removed under reduced pressure to give a crude product. The crude product was purified by column chromatography using ethyl acetate/petroleum ether (20/80, v/v) as eluent to give 4-(diphenylamino)phenylboronic acid, and the product was used in the next step directly.

Thus, the boronic acid obtained was dissolved in 300 mL of toluene and 4.059 g (34.4 mmol) of pinacol was added into the mixture. The reaction solution was refluxed with a Dean−Stark apparatus for 10 h. Then, the organic layer was separated and washed twice with water. After being dried over Na_2SO_4, the solvent was removed under reduced pressure. The crude product was purified by column chromatography using ethyl acetate/petroleum ether (10/80, v/v) as eluent to give **4** as white solid in a yield of 64% totally. ^{1}H NMR (300 MHz, $CDCl_3$, δ): 7.66 (2H, d), 7.26 (4H, m), 7.01−7.12 (8H, m), 1.33 (12H, s).

7-Bromo-9,9-dioctyl-9H-fluorene-2-carbonitrile (6). A mixture of **5** (24.08 g, 43.94 mmol) and CuCN (3.54 g, 39.55 mmol, 0.9 equiv) in NMP (100 mL) was purged with argon and refluxed overnight. Then, the reaction temperature was reduced to 120 °C and 20 g of $FeCl_3$ in 10 mL of concentrated HCl and 40 mL of H_2O were added into the dark solution. The mixture was stirred for a further 30 min. After being cooled at room temperature, the mixture was extracted with toluene (150 mL) twice and the organic layer was washed with 100 mL of 6 N HCl, water, 10% NaOH solution, and water again prior to being dried over Na_2SO_4. The solvent was then removed under reduced pressure to give a crude product. The crude product was purified by column chromatography using CH_2Cl_2/petroleum ether (20/80, v/v) as eluent, followed by recrystallization from ethanol to offer **6** as white crystals in a yield of 53%. ^{1}H NMR (300 MHz, $CDCl_3$, δ): 7.74 (1H, dd), 7.63 (3H, m), 7.52 (2H, m), 1.95 (4H, t), 1.03−1.25 (20H, m), 0.83 (6H, t), 0.55 (4H, m). FT-IR (NaCl pellets, cm^{-1}): 2928, 2854, 2223, 1611, 1458, 1376, 821. MS (EI): *m*/*e* 496, 494 (M^+).

7-(4-(Diphenylamino)phenyl)-9,9-dioctyl-9H-fluorene-2-carbonitrile (7). To a 100 mL Schlenk tube charged with **6** (1.381 g, 2.8 mmol), **4** (1.296 g, 3.5 mmol), $Pd(PPh_3)_4$ (0.161 g, 0.14 mmol), and Na_2CO_3 (2.12 g, 20 mmol) were added 50 mL of THF and 10 mL of H_2O. The mixture was frozen with liquid

N_2 and pumped to a vacuum for 20 min and then thawed with ethanol in an Ar atmosphere. The procedure above was repeated three times. The mixture was heated to 80 °C and stirred for 72 h at this temperature. After being cooled to room temperature, the mixture was diluted with 100 mL of toluene. The organic layer was separated, washed with water, and dried over anhydrous Na_2SO_4. The solvent was then removed under reduced pressure to give a crude product. The crude product was purified by column chromatography using CH_2Cl_2/petroleum ether (10/80, v/v) as eluent, followed by recrystallization from ethanol to offer **7** as yellowish green crystals in a yield of 87%. ^{1}H NMR (300 MHz, $CDCl_3$, δ): 7.74−7.79 (2H, m), 7.53−7.65 (6H, m), 7.25−7.31 (4H, m), 7.14−7.18 (6H, m), 7.05 (2H, m), 2.09 (4H, m), 1.05−1.20 (20H, m), 0.87 (6H, t), 0.62 (4H, m). ^{13}C NMR (100 MHz, $CDCl_3$, δ): 152.17, 151.64, 147.60, 145.55, 141.52, 137.96, 134.77, 131.41, 129.37, 127.92, 126.46, 125.97, 124.57, 123.78, 123.18, 121.18, 121.01, 120.19, 120.01, 109.68, 55.62, 40.21, 31.80, 29.92, 29.21, 23.80, 22.63, 14.11. FT-IR (NaCl pellets, cm^{-1}): 2926, 2854, 2223, 1593, 1515, 1494, 1465, 1375, 1281, 817, 753, 696. MS (MALDI-TOF): *m*/*z* 658.5 (M^+). Anal. Calcd for $C_{48}H_{54}N_2$: C, 87.49; H, 8.26; N, 4.25. Found: C, 87.18; H, 8.30; N, 4.07.

4,4′,4″-(7,7′,7″-(1,3,5-Triazine-2,4,6-triyl)tris(9,9-dioctyl-9H-fluorene-7,2-diyl))tris(N,N-diphenylani-line) (TFT1). This compound was prepared using a similar procedure to that used for the synthesis of **FT1**. Yellow solid. Yield of 78%. M.p.: 123 °C. ^{1}H NMR (300 MHz, $CDCl_3$, δ): 8.87 (3H, d), 8.78 (3H, s), 7.95 (3H, d), 7.88 (3H, d), 7.59−7.65 (12H, m), 7.25−7.32 (12H, m), 7.16−7.22 (18H, m), 7.06 (6H, t), 2.11−2.22 (12H, m), 1.09−1.26 (60H, m), 0.73−0.88 (30H, m). ^{13}C NMR (100 MHz, $CDCl_3$, δ): 171.90, 152.74, 151.40, 147.72, 147.32, 145.37, 140.58, 139.28, 135.41, 135.26, 129.38, 128.43, 127.94, 125.77, 124.49, 124.00, 123.33, 123.07, 121.13, 120.87, 119.81, 55.44, 40.51, 31.87, 30.15, 29.31, 23.96, 22.67, 14.12. FT-IR (NaCl pellets, cm^{-1}): 2926, 2853, 1593, 1511, 1492, 1467, 1369, 1280, 814, 752, 695. MS (MALDI-TOF): mz 1977.6 (M^+). Anal. Calcd for $C_{144}H_{162}N_6$: C, 87.49; H, 8.26; N, 4.25. Found: C, 87.28; H, 8.14; N, 4.06.

(7-Bromo-9,9-dioctyl-9H-fluoren-2-yl)trimethylsilane (8). 5.48 g (10 mmol) of **5** was dissolved in 100 mL of dry tetrahydrofuran (THF), and the solution was cooled down to −78 °C. Then, 6.9 mL (11 mmol, 1.1 equiv) of n-BuLi (1.6 M in hexane) was added through a syringe over about 30 min. After stirring for 1 h at −78 °C, 20 g (20 mmol, 2 equiv) of chlorotrimethylsilane (1 M in THF) was added. After being stirred overnight at room temperature, the reaction mixture was poured into 200 mL of water and extracted with petroleum ether. The organic layer was washed with water three times and dried over Na_2SO_4. The solvent was removed under reduced pressure to give a crude product. The crude product was purified by column chromatography using petroleum ether as eluent to give **8** as a colorless oil liquid in a yield of 94%. ^{1}H NMR (300 MHz, $CDCl_3$, δ): 7.64 (1H, d), 7.56 (1H, d), 7.42−7.50 (4H, m), 1.92 (4H, m), 1.05−1.22 (20H, m), 0.82 (6H, t), 0.61 (4H, m), 0.30 (9H, s).

(9,9-Dioctyl-7-(4,4,5,5-tetramethyl-1,3,2-dioxaborolan-2-yl)-9H-fluoren-2-yl)trimethylsilane (9). This compound was prepared using a similar procedure to that used for the synthesis of **4** in a yield of 74%. ^{1}H NMR (300 MHz, $CDCl_3$, δ): 7.80 (1H, d), 7.69−7.74 (3H, m), 7.46−7.50 (2H, m), 1.97 (4H, m), 1.03−1.21 (20H, m), 0.81 (6H, t), 0.60 (4H, m), 0.31 (9H, s).

9,9,9′,9′-Tetraoctyl-7′-(trimethylsilyl)-9H,9′H-2,2′-bifluorene-7-carbonitrile (10). This compound was prepared using a similar procedure to that used for the synthesis of **7** in a yield of 87%. ^{1}H NMR (300 MHz, $CDCl_3$, δ): 7.78−7.83 (2H, m), 7.60−7.74 (8H, m), 7.49−7.53 (2H, m), 2.02 (8H, m), 1.07−1.25 (40H, m), 0.63−0.87 (20H, m), 0.31 (9H, s).

7′-Iodo-9,9,9′,9′-tetraoctyl-9H,9′H-2,2′-bifluorene-7-carbonitrile (11). 1.89 g (2.16 mmol) of **10** was dissolved in 25 mL of dry dichloromethane (DCM), and the solution was cooled down to 0 °C. Then, 2.59 mL (2.59 mmol, 1.2 equiv) of ICl (1 M in DCM) was added through a syringe over about 20 min. After being stirred for 2 h at room temperature, the reaction mixture was poured into 200 mL of 15% aqueous $NaHSO_3$ solution and extracted with DCM. The organic layer was washed with water three times and dried over Na_2SO_4. The solvent was removed under reduced pressure to give a crude product. The crude product was purified by column chromatography using CH_2Cl_2/petroleum ether (10/80, v/v) as eluent, followed by recrystallization from chloroform/ethanol to offer **11** as a white solid in a yield of 100%. ^{1}H NMR (300 MHz, $CDCl_3$, δ): 7.78−7.83 (2H, m), 7.60−7.74 (8H, m), 7.49−7.53 (2H, m), 2.02 (8H, m), 1.07−1.25 (40H, m), 0.63−0.87 (20H, m), 0.31 (9H, s). ^{13}C NMR (100 MHz, $CDCl_3$, δ): 153.40, 152.22, 151.66, 151.01, 145.35, 142.27, 140.51, 140.25, 139.76, 138.38, 135.94, 132.14, 131.38, 126.61, 126.49, 126.36, 121.51, 121.38, 121.08, 120.25, 120.12, 119.88, 109.82, 92.68, 55.63, 55.48, 40.18, 40.07, 31.75, 31.72, 29.89, 29.85, 29.14, 23.77, 23.73, 22.59, 22.56, 14.03. FT-IR (NaCl pellets, cm^{-1}): 2926, 2854, 2222, 1609, 1455, 1402, 1377, 1261, 1002, 892, 811, 755, 722. MS (MALDI-TOF): *m*/*z* 803.5 $(M-I)^+$. Anal. Calcd for $C_{59}H_{80}IN$: C, 76.18; H, 8.67; N, 1.51. Found: C, 76.63; H, 8.68; N, 1.49.

7′-(4-(Diphenylamino)phenyl)-9,9,9′,9′-tetraoctyl-9H,9′H-2,2′-bifluorene-7-carbonitrile (12). This compound was prepared using a similar procedure to that used for the synthesis of **7** in a yield of 69%. ^{1}H NMR (300 MHz, $CDCl_3$, δ): 7.77−7.84 (4H, m), 7.56−7.71 (10H, m), 7.25−7.31 (4H, m), 7.15−7.19 (6H, m), 7.06 (2H, m), 2.05 (8H, m), 1.01−1.25 (40H, m), 0.58−0.83 (20H, m). ^{13}C NMR (100 MHz, $CDCl_3$, δ): 152.19, 151.82, 151.67, 147.68, 147.13, 145.44, 142.52, 140.57, 139.67, 139.46, 138.21, 135.51, 131.37, 129.28, 127.79, 126.59, 126.48, 126.23, 125.60, 124.38, 123.98, 122.94, 121.49, 121.42, 121.06, 121.00, 120.21, 120.07, 119.94, 109.72, 55.62, 55.30, 40.39, 40.10, 31.76, 31.73, 29.99, 29.87, 29.70, 29.18, 29.15, 23.83, 23.79, 22.57, 14.04. FT-IR (NaCl pellets, cm^{-1}): 3035, 2926, 2854, 2224, 1593, 1515, 1493, 1461, 1377, 1278, 815, 753, 695. MS (MALDI-TOF): *m*/*z* 1047.2 (M^+). Anal. Calcd for $C_{77}H_{94}N_2$: C, 88.28; H, 9.04; N, 2.67. Found: C, 88.02; H, 9.34; N, 2.25.

TFT2. This compound was prepared using a similar procedure to that used for the synthesis of **FT1** in a yield of 40% as a yellow solid. M.p.: 135 °C. ^{1}H NMR (300 MHz, $CDCl_3$, δ): 8.90 (3H, d), 8.82 (3H, s), 8.01 (3H, d), 7.93 (3H, d), 7.58−7.84 (30H, m), 7.25−7.32 (12H, m), 7.16−7.21 (18H, m), 7.05 (6H, t), 2.08−2.24 (24H, m), 1.03−1.27 (120H, m), 0.71−0.89 (60H, m). ^{13}C NMR (100 MHz, $CDCl_3$, δ): 171.90, 152.76, 151.78, 151.73, 151.43, 147.70, 147.08, 145.25, 141.59, 140.29, 140.19, 139.63, 139.54, 135.62, 135.31, 129.28, 128.40, 127.79, 126.34, 126.21, 125.57, 124.37, 124.02, 123.38, 122.92, 121.58, 121.49, 121.00, 120.77, 120.02, 119.92, 55.43, 55.30, 40.43, 31.80, 30.08, 30.04, 29.25, 29.22, 23.94, 23.87, 22.59, 14.06, 14.03. FT-IR (NaCl pellets, cm^{-1}): 2926, 2854, 1592, 1515, 1494, 1460, 1370, 1280, 814, 752, 696. MS (MALDI-TOF): *m*/*z* 3142.7 (M^+). Anal. Calcd for $C_{231}H_{282}N_6$: C, 88.28; H, 9.04; N, 2.67. Found: C, 88.46; H, 9.24; N, 2.31.

13. This compound was prepared using a similar procedure to that used for the synthesis of **7** in a yield of 78%. ^{1}H NMR (300 MHz, $CDCl_3$, δ): 7.78−7.84 (5H, m), 7.63−7.74 (11H,

m), 7.50−7.53 (2H, m), 2.00−2.13 (12H, m), 1.07−1.25 (60H, m), 0.59−0.83 (30H, m), 0.33 (9H, s).

14. This compound was prepared using a similar procedure to that used for the synthesis of **11** in a yield of 99%. ^{1}H NMR (300 MHz, $CDCl_3$, δ): 7.80−7.84 (4H, m), 7.72−7.77 (2H, m), 7.60−7.69 (11H, m), 7.49 (1H, d), 1.99−2.12 (12H, m), 1.01−1.24 (60H, m), 0.59−0.84 (20H, m), 0.31 (9H, s). FT-IR (NaCl pellets, cm^{-1}): 2927, 2854, 2224, 1608, 1459, 1402, 1377, 1259, 1001, 887, 817, 756, 722. MS (MALDI-TOF): *m/z* 1318.1 (M^+), 1192.2 $(M-I)^+$. Anal. Calcd for $C_{88}H_{120}IN$: C, 80.14; H, 9.17; N, 1.06. Found: C, 80.36; H, 9.12; N, 0.87.

15. This compound was prepared using a similar procedure to that used for the synthesis of **7** in a yield of 63%. ^{1}H NMR (300 MHz, $CDCl_3$, δ): 7.77−7.85 (6H, m), 7.64−7.73 (10H, m), 7.57−7.60 (4H, m), 7.25−7.31 (4H, m), 7.15−7.20 (6H, m), 7.05 (2H, m), 2.08 (12H, m), 1.02−1.26 (60H, m), 0.60−0.88 (30H, m). ^{13}C NMR (100 MHz, $CDCl_3$, δ): 152.21, 151.90, 151.79, 151.73, 151.68, 147.69, 147.07, 145.44, 142.52, 140.72, 140.53, 140.28, 140.14, 139.79, 139.64, 139.49, 138.24, 135.62, 131.38, 129.27, 127.78, 126.60, 126.49, 126.27, 126.19, 126.11, 124.36, 124.02, 122.91, 121.51, 121.07, 120.99, 120.22, 120.03, 119.88, 109.73, 55.64, 55.36, 55. 27, 40.42, 40.33, 40.10, 31.77, 31.74, 30.02, 29.99, 29.87, 29.19, 23.85, 23.79, 22.57, 14.04. FT-IR (NaCl pellets, cm^{-1}): 2926, 2854, 2224, 1593, 1515, 1494, 1460, 1377, 1280, 814, 753, 696. MS (MALDI-TOF): *m/z* 1436.0 (M^+). Anal. Calcd for $C_{106}H_{134}N_2$: C, 88.65; H, 9.40; N, 1.95. Found: C, 88.02; H, 9.32; N, 1.72.

TFT3. This compound was prepared using a similar procedure to that used for the synthesis of **FT1** in a yield of 38% as a yellow solid. M.p.: 168 °C. ^{1}H NMR (300 MHz, $CDCl_3$, δ): 8.91 (3H, d), 8.83 (3H, s), 8.03 (3H, m), 7.95 (3H, m), 7.44−7.87 (48H, m), 7.25−7.32 (12H, m), 7.16−7.23 (18H, m), 7.05 (6H, m), 2.08−2.26 (36H, m), 1.05−1.28 (180H, m), 0.69−0.89 (90H, m). ^{13}C NMR (100 MHz, $CDCl_3$, δ): 171.92, 152.79, 152.02, 151.85, 151.75, 151.46, 150.10, 147.72, 147.08, 145.27, 141.60, 141.51, 141.38, 140.61, 140.54, 140.44, 140.29, 140.06, 139.86, 139.64, 139.57, 139.43, 135.69, 135.34, 129.29, 128.43, 127.80, 126.37, 126.20, 125.56, 124.37, 124.07, 123.41, 123.25, 123.15, 122.92, 121.55, 120.96, 120.80, 120.01, 119.91, 118.41, 118.30, 55.46, 55.31, 55.09, 55.02, 40.42, 31.82, 30.11, 29.27, 23.98, 22.61, 14.08. FT-IR (NaCl pellets, cm^{-1}): 2926, 2852, 1591, 1515, 1493, 1461, 1371, 1277, 814, 752, 695. Anal. Calcd for $C_{318}H_{402}N_6$: C, 88.65; H, 9.40; N, 1.95. Found: C, 88.62; H, 9.27; N, 2.34.

Measurement of Nonlinear Optical Properties. For the study on the nonlinear optical properties of these new materials, we employed a femtosecond laser system consisting of a mode locked Ti:sapphire oscillator (Tsunami, Spectra Physics) and a regenerative amplifier (spitfire). The average output power was about 90 mW with a repetition rate of 1 kHz, a pulse duration of 140 fs, and the wavelength at 800 nm. We used the open-aperture *Z*-scan technique to measure the TPA cross section and closed aperture for the third-order nonlinear refractivity. The laser beam with 1.3 mJ pulse energy was focused on the solution in a 1 mm cell by a lens of 10 cm focal length and the transmitted light, after the sample was collected by a photodiode detector connected with a lock-in amplifier.

OLED Device Fabrication and Measurement. Indium tin oxide (ITO)-coated glass substrates were cleaned by ultrasonically washing in isopropyl alcohol, detergent solution, deionized water, and isopropyl alcohol successively before being dried under N_2 flushing and UV-ozone treatment. Then, PEDOT:PSS was spin-coated onto the ITO glass from its aqueous solution and dried at 150 °C for 20 min in air. The emitting layer was then spin-coated on the top of the PEDOT:PSS layer from a toluene solution of **TFT1** (or **TFT2** and **TFT3**) (15 mg/mL), followed by drying at 60 °C for 2 h in a glovebox. The electron transport layer, electron injection layer (LiF), and the cathode Al were sequentially evaporated onto the emitting layer. During the deposition, the thickness of the layers was monitored by an oscillating quartz crystal and optimized device to device. The properties of the devices were measured at room temperature in air. The EL spectra were recorded on a photometer PR 705.

SCHEME 1: Molecular Structures of the Star-Shaped Oligomers

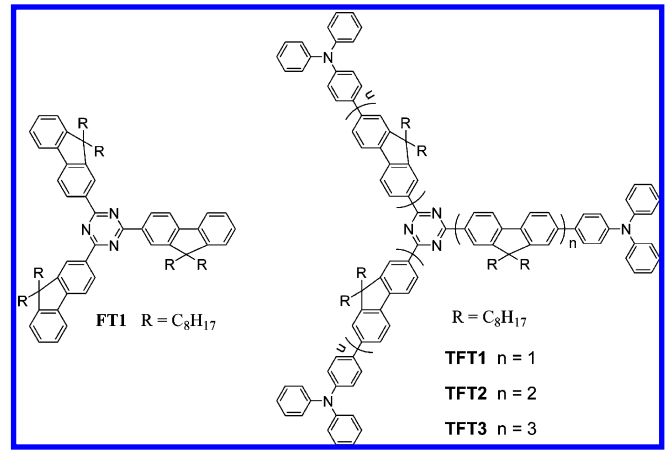

Results and Discussion

Synthesis and Characterization. Molecular structures of the star-shaped molecules are shown in Scheme 1. **FT1** is a molecule centered with the electron-withdrawing 1,3,5-triazine group and armed with three fluorene units, whereas **TFT1**, **TFT2**, and **TFT3** have bridges made of different numbers of fluorene units between the 1,3,5-triazine core and electron-donating triphenylamine peripherals. Synthesis of 1,3,5-triazine derivatives is most commonly started with nucleophilic aromatic substitution of cyanuric halides, followed by further modifications.[14a,d] The problem with this method is that in every step there are three reacting sites, which makes the purification procedure very tedious. In this contribution, we adopted a convergent synthetic strategy and left 1,3,5-triazine formation as the last step, making the whole synthesis more efficient.

Synthetic routes of these molecules are shown in Schemes 2 and 3. The synthesis started from cyanization of 2-bromo-9,9-dioctylfluorene (**1**) to give the cyano compound **2** in a yield of 68%. Then, compound **2** underwent a trimerization reaction under strong acid conditions with trifluoromethanesulfonic acid in chloroform to afford the star-shaped compound **FT1** in a high yield of 91%.

For the first generation D-π-A type compound **TFT1**, 2,7-dibromo-9,9-dioctylfluorene **5** was used as the starting material to undergo a monocyanization reaction using 0.9 equivalent CuCN to give compound **6**. Meanwhile, borylation of 4-bromo-*N*,*N*-diphenylbenzenamine **3** gave rise to the boronic easter compound **4**. Suzuki coupling between **4** and**6** gave the triazine precursor **7** in a yield of 86%. With the same conditions as the synthesis of **FT1**, **TFT1** was obtained as yellowish solid in a reasonable yield (78%). The key point of the trimerization reaction was the feeding sequence, with adding the reactant solution to the acid necessary for better yield.[13a]

Borolane compound **9** was synthesized through two steps from compound **5**, monoprotection by TMS and borylation.

SCHEME 2: Synthesis of Star-Shaped Oligomers FT1 and TFT1

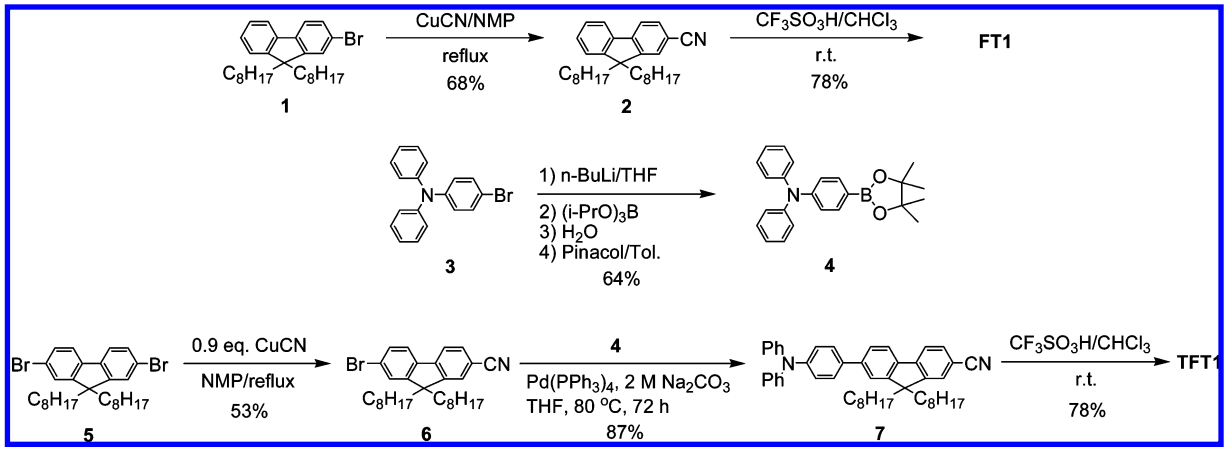

SCHEME 3: Synthesis of Star-Shaped Oligomers TFT2 and TFT3

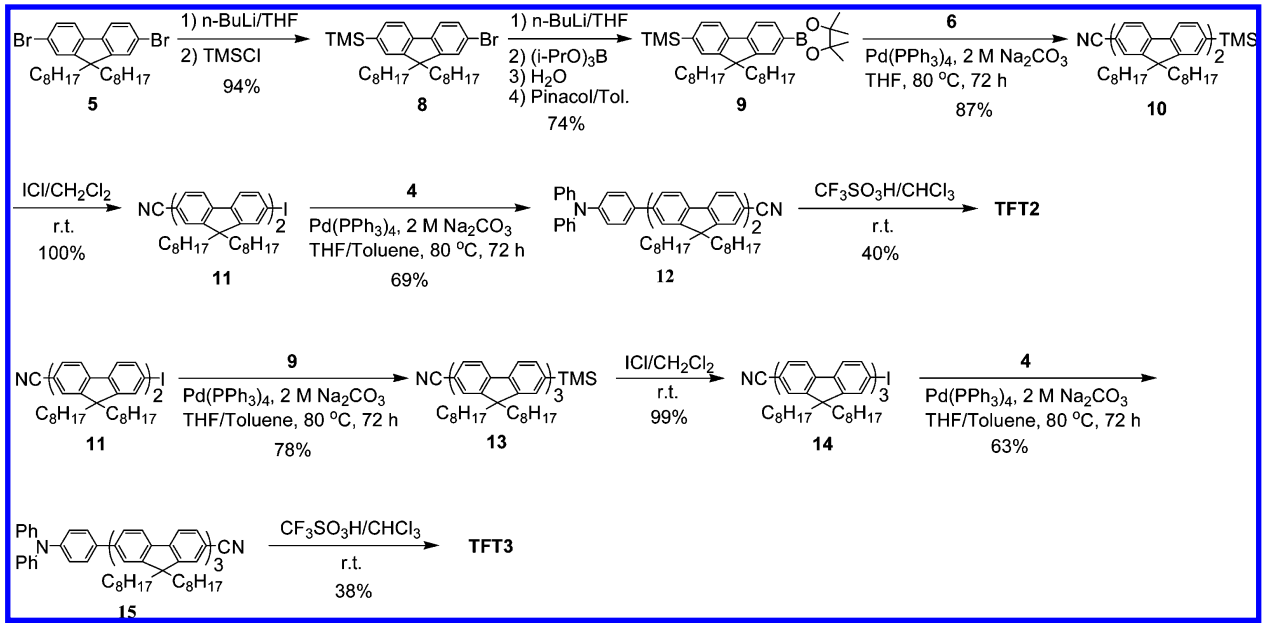

Then, compound **9** underwent a Suzuki coupling reaction with compound **6** to afford the compound **10**, which was subsequently converted to compound **11** through an iodination reaction in a quantative yield. Another Suzuki reaction was employed to synthesize the second generation triazine precursor **12**, followed by the cyclization to make **TFT2**.

Suzuki coupling reaction between the iodo compound **11** and the boronic easter compound **9** gave rise to the trisfluorene compound **13**, followed by an iodination reaction to produce compound **14**. Suzuki coupling between **14** and **4** gave the third generation triazine precursor **15**, which then underwent a trimerization reaction to give **TFT3**.

All four final compounds dissolved readily in common organic solvents such as dichloromethane, chloroform, toluene, and tetrahydrofuran, which allowed us to do conventional characterization by normal spectroscopic techniques. The identity and purity of all new compounds were confirmed by various methods, such as ^{1}H NMR, ^{13}C NMR spectra, mass spectrometry, and elemental analysis, as detailed in the experimental part. The ^{13}C NMR of the star-shaped molecules showed characteristic signals of the 1,3,5-triazine unit around 172 ppm. Mass spectra of **TFT3** were not able to be obtained after several tries, so gel permeation chromatography (GPC) was used to further characterize these molecules, as shown in Figure 1 and Table 1. The GPC results showed that the molecular weight of these star-shaped molecules was monodispersed and correlated well with their calculated molecular weight.

Thermogravimetric analysis (TGA) performed in a nitrogen atmosphere showed good thermal stability of the star-shaped compounds (Figure 2 and Table 1). The 5% weight loss temperatures of the star-shaped compounds were all more than 425 °C with the best 439 °C of **TFT1**.

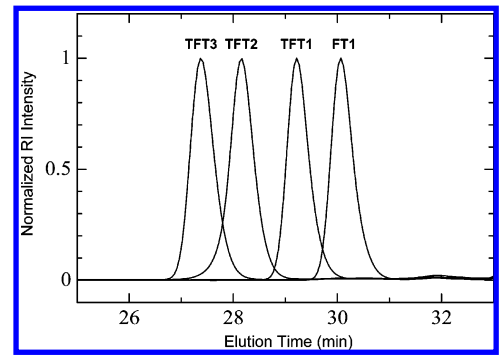

Figure 1. GPC traces of the star-shaped oligomers.

TABLE 1: Summary of the Experimental Data of the Star-Shaped Oligomers

			$\lambda_{SPA}^{max\ a}$ (nm)						$\lambda_{SPEF}^{max\ b}$ (nm)					
compound	M_n (PDI)[c]	T_d[d] (°C)	CYC	TOL	THF (lg ε[e])	DCM	DMF	film	CYC	TOL (Φ_{PL})[f]	THF	DCM	DMF	film
FT1	1500 (1.02)	425	333/351	336/352	351 (4.96)	351	352	366	360/378	385 (0.08)	393	401	413	394
TFT1	2600 (1.01)	439	387	392	391 (5.18)	391	395	399	435/456	465 (0.83)	522	544	574	479
TFT2	4200 (1.01)	436	385	388	388 (5.50)	389	393	394	429	445 (0.93)	508	544	453	471
TFT3	5600 (1.01)	433	373	375	378 (5.51)	379	381	378	423	431 (0.99)	461	473	452	464

[a] λ_{SPA}^{max}, maximum single-photon absorption wavelength in different solutions (cyclohaxane, CYC; toluene, TOL; tetrahydrofuran, THF; dichloromethane, DCM; *N*,*N*-dimethylformamide, DMF) and solid state (film). [b] λ_{SPEF}^{max}, maximum single-photon excited fluorescence wavelength in different solutions and solid state. [c] Determined by GPC using polystyrene as reference and THF as elute. [d] 5% weight loss temperature determined by TGA. [e] Molar extinction coefficient. [f] Photoluminescence quantum yield determined in toluene solutions with a 0.5 M H_2SO_4 solution of quinine (10^{-5} M, $\Phi_{PL} = 0.55$) as reference.

Single-Photon Photophysical and Electrochemical Properties. The single-photon excited absorption and fluorescence properties of the star-shaped compounds are summarized in Table 1. The single-photon absorption (SPA) and single-photon excited fluorescence (SPEF) spectra were measured in various solvents with different polarities, which ranged from nonpolar cyclohexane (dielectric constant $D_k = 2.02$), medium polar toluene ($D_k = 2.38$), THF ($D_k = 7.5$), and DCM ($D_k = 9.1$) to highly polar DMF ($D_k = 38$), to investigate the influence of solvent polarity on the optical properties of these triazine based compounds.

The SPA spectra of all of the star-shaped oligomers were slightly changed in solvents of different polarities, with the SPA maxima (λ_{SPA}^{max}) located at around 351 nm for **FT1**, 393 nm for **TFT1**, 390 nm for **TFT2**, and 378 nm for **TFT3** (Table 1 and Figure 3). In THF solutions, molar absorption coefficients (ε) of the star-shaped compounds were measured. The ε value was increased from 9.12×10^4 for **FT1** to 1.51×10^5 for **TFT1** with the addition of the electron donating group of triphenylamine, and it was further enhanced by the expansion of the π-spacer, with **TFT2** having a ε value of 3.16×10^5 and **TFT3** of 3.24×10^5.

In contrast to the absorption process, SPEF of all the star-shaped compounds exhibited solvatochromism in different solvents. With increasing solvent polarity, the SPEF maxima (λ_{SPEF}^{max}) showed bathochromic shifts of different extent according to each specific compound. **FT1** showed two emission peaks in cyclohexane, located at 360 and 378 nm; however, in the other four more polar solvents, there was only one emission peak left and λ_{SPEF}^{max} red-shifted regularly with the increasing solvent polarity. In detail, the maximum emission wavelength moved from 360 nm in cyclohexane to 413 nm in DMF. In the meanwhile, the Stokes shifts between the absorption and emission of **FT1** in the solvents cyclohexane, toluene, THF, DCM, and DMF were 9, 34, 42, 50, and 61 nm, respectively. The solvatochromism is caused by photoinduced intramolecular charge transfer (ICT) in the excited state. Such chromic behavior is associated with the stabilization of the polar emissive excited states by the polar solvents.[9a] Similar results have been observed in linear donor−acceptor oligomers.[20]

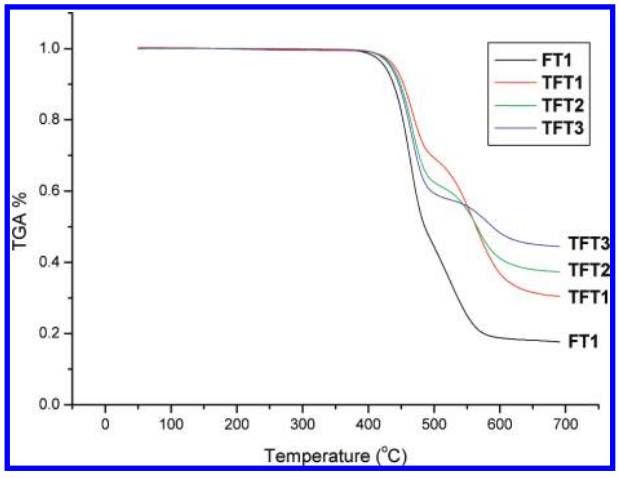

Figure 2. TGA curves of the star-shaped oligomers.

Compared with **FT1**, the SPFE spectra of the D-π-A molecule **TFT1** showed a much stronger solvatochromism phenomenon. The SPEF maximum of **TFT1** shifted from 435 nm in cyclohaxane to 574 nm in DMF, which was a 139 nm change, while, under the same circumstances, there was only a 53 nm red-shift for **FT1**. The enhancement of solvatochromism indicated that the attachment of the strong electron-donating triphenylamine group significantly increased the ICT effects in the D-π-A molecule. The Stokes shifts between the absorption and emission of **TFT1** in the solvents cyclohexane, toluene, THF, DCM, and DMF were 48, 73, 131, 153, and 179 nm, respectively. The SPEF spectra of **TFT2** and **TFT3** were also measured in different solvents, and they basically showed the same solvatochromism behaviors, except for the abnormality in DMF due to poor solubility.

As shown in Table 1, in the same solvent, both λ_{SPA}^{max} and λ_{SPEF}^{max} values of the star-shaped compounds could be sequenced as **TFT1** > **TFT2** > **TFT3** > **FT1**. For example, in toluene solutions, the λ_{SPA}^{max} values of **FT1**, **TFT1**, **TFT2**, and **TFT3** were 352, 392, 388, and 375 nm and the λ_{SPEF}^{max} values were 385, 465, 445, and 431 nm, respectively, suggesting that the addition of electron donating groups could effectively lower the band gap of the molecules and the expansion of the fluorenyl bridge could contrarily increase the band gap, which was not surprising because of the high band gap properties of fluorene based materials. Photoluminescence quantum yields (Φ_{PL}) of the star-shaped oligomers in toluene solutions were measured with a 0.5 M H_2SO_4 solution of quinine (10^{-5} M, $\Phi_{PL} = 0.55$) as reference. The Φ_{PL} of **TFT1** was more than 10 times of that of **FT1** (the emission of **FT1** fell in the ultraviolet region, so the quinine solution was not a very good reference), and when the number of the bridging fluorene units was increased, the Φ_{PL} value was further enhanced, up to 99% for **TFT3**. Normally, the ICT process in a molecule leads to the decrease of Φ_{PL},[8g] so the results here also evidenced the weakening of the ICT effects as the length of the oligomeric fluorene arms increased.

In order to investigate the condensed optical properties of the star-shaped oligomers, we studied their SPA and SPEF behaviors in the solid states, as shown in Table 1 and Figure 4. Uniformly smooth thin films were prepared on glass substrates by spin-coating from toluene solutions. The SPA maximum

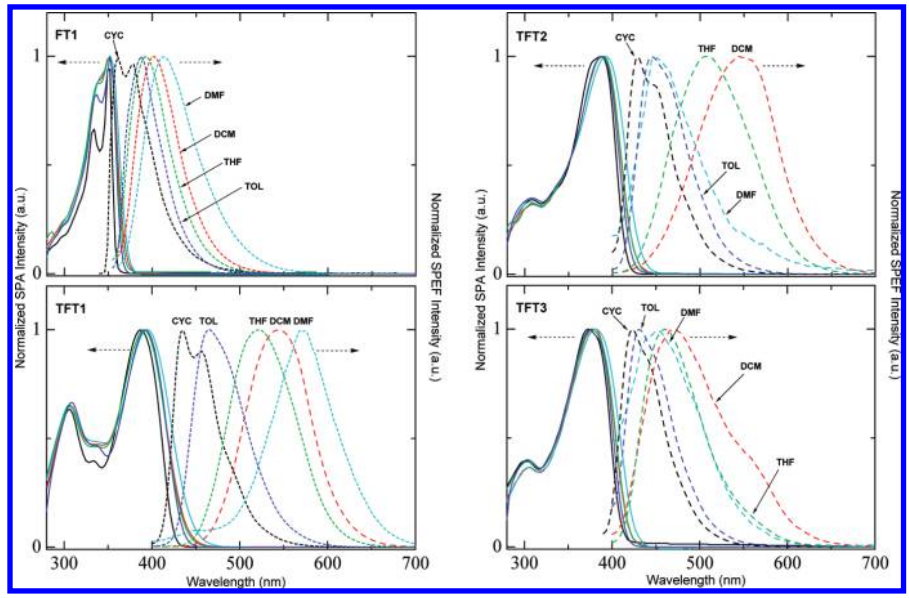

Figure 3. SPA (solid lines) and SPEF (dashed lines) spectra of the star-shaped oligomers in different solvents (CYC, black; TOL, blue; THF, green; DCM, red; DMF, cyan).

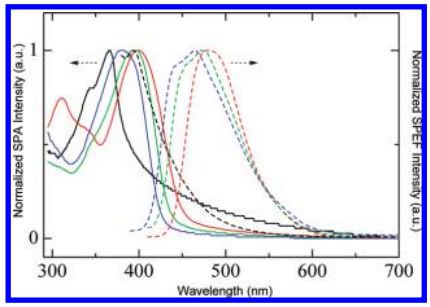

Figure 4. SPA (solid lines) and SPEF (dashed lines) spectra of the star-shaped oligomers in the solid states (**FT1**, black; **TFT1**, red; **TFT2**, green; **TFT3**, blue).

wavelength of **FT1** film was 366 nm, about 15 nm red-shifted from the λ_{SPA}^{max} value in solution, while the D-π-A compounds **TFT1**−**3** showed almost the same λ_{SPA}^{max} values in both solutions and solid states. These results indicated that the attachment of the nonplanar triphenylamine group could effectively suppress the solid state stacking. All of the films of **FT1** and **TFT1**−**3** were intensively fluorescent under UV−vis excitation, with λ_{SPEF}^{max} at 394, 479, 471, and 464 nm, respectively. Annealing experiments were employed to test the fluorescence stability of the oligomers in films, and it was found that all of the D-π-A compounds showed almost unchanged fluorescent properties after thermal annealing, which was favorable for the overall stability of the electroluminescent devices.

The optical band gaps of these oligomers were estimated from the onset wavelength of their solid state optical absorption, as summarized in Table 2. The band gap of **FT1** was 3.16 eV, and that of **TFT1** was effectively lowered to 2.75 eV due to the strong ICT effect. The band gaps of **TFT2** (2.83 eV) and **TFT3** (2.90 eV) were increased gradually as the π-spacer became longer. To further study the effect of arm length on the electrochemical properties of the D-π-A star-shaped oligomers, cyclic voltammetry (CV) was performed with the cast films on ITO glass, as shown in the Supporting Information (Figure S15). The potentials were reported relative to an internal Fc^+/Fc standard with a scan rate of 0.1 V/s. All oligomers exhibited reversible electrochemical oxidation behavior with the p-doping onset located at 0.49, 0.53, and 0.54 eV versus Ag^+/Ag, respectively. The highest occupied molecular orbital (HOMO) and lowest unoccupied molecular orbital (LUMO) energy levels of these oligomers were then calculated and shown in Table 2. In OLED applications, the work function of commonly used anode material ITO is 4.8 eV and the work function of widely used cathode Al is 3.7 eV; thus, compared to **TFT2** and **TFT3**, **TFT1** has better energy level matching with the electrodes, which would be favorable for hole and electron transporting to afford better electroluminescence properties.

Nonlinear Optical and Two-Photon Absorption and Emission Properties. The nonlinear optical properties of the D-π-A oligomers were measured by closed-aperture and open-aperture *Z*-scan techniques. As shown in Figure 5, both **TFT1** and **TFT2**

TABLE 2: Summary of Redox and Nonlinear Optical Data of the Star-Shaped Oligomers

compound	E_g^{opt} [a] (eV)	E_{ox}^{onset} [b] (V)	E_{HOMO} [c] (eV)	E_{LUMO} [d] (eV)	n_2 [e] (esu)	λ_{TPEF}^{max} [f] (nm)	σ [g] (GM)
FT1	3.16						
TFT1	2.75	0.49	−5.29	−2.54	4.14×10^{-12}	527	234
TFT2	2.83	0.53	−5.33	−2.50	2.48×10^{-12}	514	196
TFT3	2.90	0.54	−5.34	−2.44		470	189

[a] Estimated from the absorption onset of the oligomer thin films. [b] Determined by CV with reference to (0.10 M $AgNO_3$)/Ag. [c] Determined from $E_{HOMO} = -(E_{ox}^{onset} + 4.8)$ (eV). [d] Calculated from $E_{LUMO} = E_{HOMO} + E_g^{opt}$. [e] Nonlinear refractive index measured by the closed-aperture *Z*-scan technique. [f] Two-photon excited fluorescence maximum wavelength excited by 800 nm lasers in THF solutions. [g] Two-photon absorption cross sections measured by the open-aperture *Z*-scan technique upon excitation of 800 nm laser pulses with a pulse width of 140 fs in 5×10^{-3} M THF solutions. 1 GM = 1×10^{-50} cm^4 s per photon per molecule.

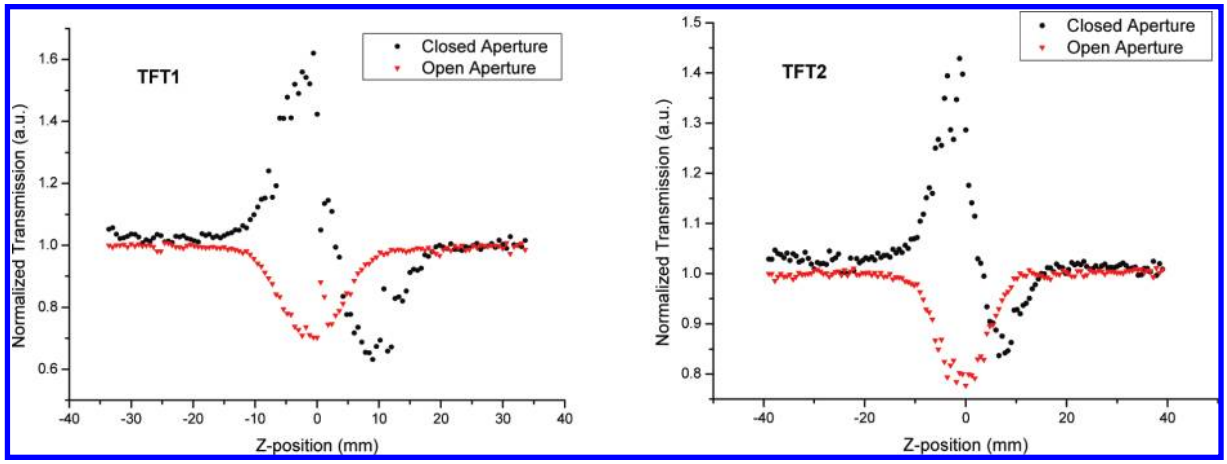

Figure 5. Normalized closed- and open-aperture *Z*-scan traces of **TFT1** and **TFT2** in THF solutions.

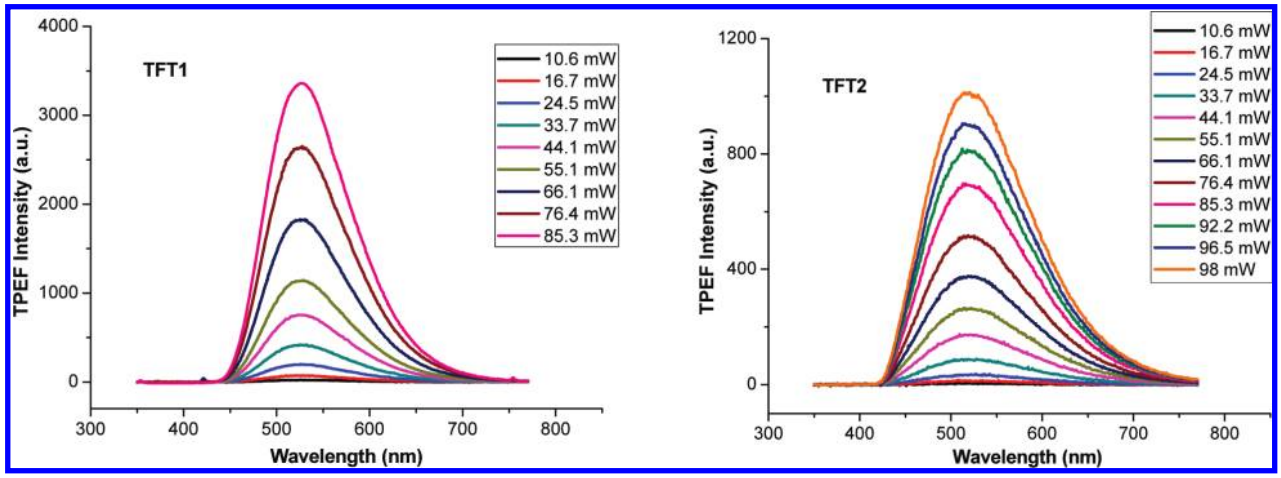

Figure 6. TPEF spectra of **TFT1** and **TFT2** in THF solutions at different average laser powers.

exhibited active nonlinear absorption and refraction behaviors. Peak−valley characteristics were shown in closed-aperture *Z*-scan measurement, indicating negative nonlinear refraction or self-defocusing effect. Using carbon disulfide (CS_2) as a reference nonlinear material ($n_2[CS_2] = 1.3 \times 10^{-11}$ esu),[21] the third-order nonlinear refractive indices (n_2) of **TFT1** and **TFT2** in THF solutions were calculated to be 4.14×10^{-12} and 2.48×10^{-12} esu, respectively. It was reported[22] that the n_2 value of poly(9,9-dioctylfluorene) (PFO) was 2.04×10^{-12} esu. Compared with **TFT2** and PFO, **TFT1** showed higher nonlinear refractivity, which could be attributed to the stronger ICT effect in the molecule.

Two-photon excited fluorescence (TPEF) spectra of the oligomers **TFT1**−**3** were recorded in THF solution at room temperature (Figure 6). Upon excitation of 800 nm laser pulses with a pulse width of 140 fs, all of the oligomers emitted extensive frequency upconverted fluorescence with the maximum TPEF wavelength (λ_{TPEF}^{max}) at 527 nm for **TFT1**, 514 nm for **TFT2**, and 470 nm for **TFT3**. As shown in Figure 7, the output intensity of two-photon excited fluorescence is linearly dependent on the square of the input laser intensity, indicating the occurrence of two-photon absorption (TPA). λ_{TPEF}^{max} of **TFT1**−**3** shifted to longer wavelength by 5−9 nm compared with their maximum SPEF wavelength (Tables 1 and 2). The red-shift could be attributed to the reabsorption of the fluorescence under more concentrated solution conditions (5×10^{-3} to 1×10^{-5} M).

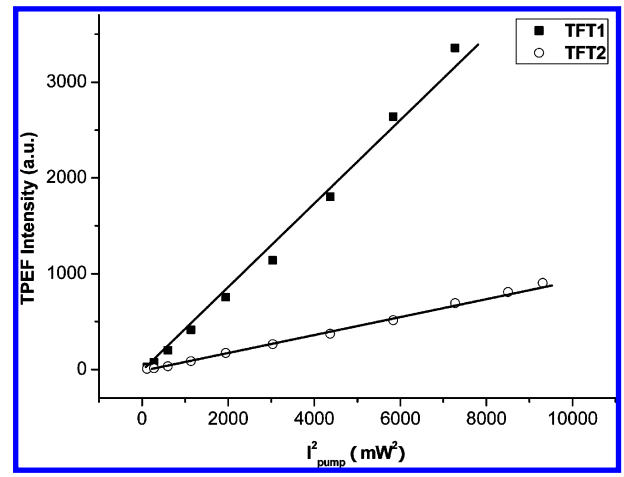

Figure 7. Linear dependence of peak fluorescence intensity on the square of the excitation powers.

TPA cross sections of the D-π-A oligomers **TFT1**−**3** were measured by open-aperture *Z*-scan experiments performed with a femtosecond 800 nm laser source. As summarized in Table 2, the TPA cross sections of **TFT1**−**3** were 234, 196, and 189 GM, respectively, which were higher than the reported cross section value of triazine derivative AF-450 (137 GM) measured under the excitation of the 790 nm laser.[15] These results indicated that the triphenylamine donor part in **TFT1**−**3** could

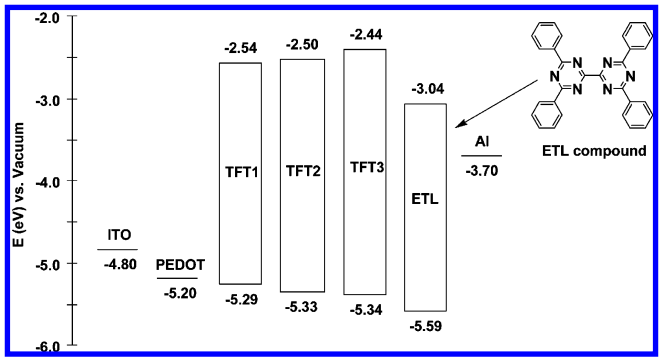

Figure 8. Schematic energy level diagram of the OLED devices and molecular structure of the ETL material. The energy level data were derived from CV and UV−vis absorption data.

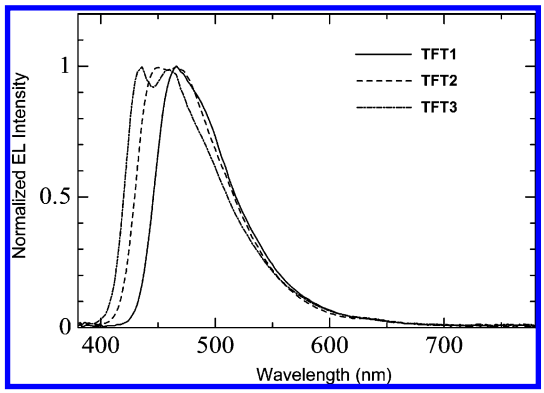

Figure 9. EL spectra of the devices with the star-shaped D-π-A oligomers as active layers (**TFT1**, solid; **TFT2**, dash; **TFT3**, dash dot).

supply stronger ICT effects than the diphenylamine counterpart in AF-450 and, within the **TFT** series, **TFT1** had the strongest nonlinear TPA ability.

Electroluminescent Properties. The star-shaped D-π-A oligomers can be easily deposited as thin films by spin-coating, and OLED devices with **TFT1**−**3** as active layers were fabricated with a configuration of ITO/PEDOT:PSS/oligomer/ETL/LiF/Al. In these devices, PEDOT:PSS was employed as the hole injection material and a bitriazine compound developed by our group[12c] was used as the electron-transporting layer (ETL) to improve electron-transporting ability and avoid using active metals such as calcium. The energy diagram of these devices was shown in Figure 8. Incorporation of an ETL could lower the electron transporting barrier between the emitting layer and the cathode. All of the electroluminescent (EL) spectra of the devices based on **TFT1**−**3**, shown in Figure 9, were similar to the corresponding solid state photoluminescent spectra of **TFT1**−**3**, indicating that holes from the anode and electrons from the cathode were combined in the active layer and the light was indeed emitted from the oligomers as expected.

As shown in Table 3, all of the devices had very low turn-on voltages compared with OLEDs fabricated by vacuum evaporation. The luminance versus operation voltage ($L-V$) and current density versus operation voltage ($J-V$) curves of the devices were shown in Figure 10. The device using **TFT1** as an emitting material showed a maximum luminance of 3093 cd/m^2 and a current efficiency of 1.47 cd/A at a relatively low driving voltage of 7.5 V, while the devices based on **TFT2** and **TFT3** exhibited less efficient electroluminescence. The reason why **TFT1** showed the best EL properties could be ascribed to easier electron and hole transportation and more balanced charge recombination. The device performances obtained here will likely be improved by optimizing the device conditions, such as varying the thickness of the active layers, the electron transport materials or the cathodes having been used.

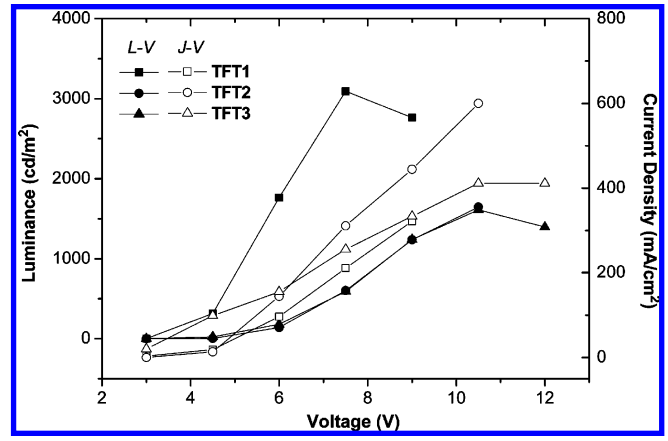

Figure 10. $L-V$ and $J-V$ curves of the OLED devices based on star-shaped D-π-A oligomers.

Conclusions

1,3,5-Triazine based star-shaped oligomer **FT1** and three generations of highly soluble donor-π-acceptor compounds, **TFT1**, **TFT2**, and **TFT3**, were prepared through an efficient convergent synthetic strategy, and their photophysical and electrochemical properties were characterized, which showed distinct correlations with their specific structures. Closed-aperture and open-aperture Z-scan measurements showed that the D-π-A oligomers were both nonlinear refraction and nonlinear absorption active. **TFT1** showed a high nonlinear refractive index of 4.14×10^{-12} esu in THF solution with an excitation wavelength of 800 nm. Among the oligomers, **TFT1** exhibited the largest two-photon absorption cross section of 234 GM under an 800 nm laser irradiation with a pulse duration of 140 fs due to the strongest ICT effect. All of the D-π-A oligomers **TFT1**−**3** showed frequency up-converted two-photon excited fluorescence with λ_{TPEF}^{max} located at 527, 514, and 470 nm, respectively. OLED devices using the spin-coated films of these oligomers as an active layer showed intensive blue electroluminescence and a

TABLE 3: Summary of the OLED Device Data of the Star-Shaped Oligomers

compound	λ_{EL}^{max} [a] (nm)	turn-on voltage[b] (V)	drive voltage[c] (V)	current density[c] (mA/cm^2)	luminance[c] (cd/m^2)	current efficiency[c] (cd/A)	power efficiency[c] (lm/w)
TFT1	466	3.0	7.5	211	3093	1.47	0.61
TFT2	450/466	3.5	10.5	600	1647	0.27	0.08
TFT3	436/460	3.5	10.5	411	1610	0.39	0.12

[a] Maximum electroluminescent wavelength of the OLED devices. [b] Voltage when the luminance is visible. [c] Measurement conditions and device performances at the maximum luminance.

maximum luminance of 3093 cd/m^2 at a current efficiency of 1.47 cd/A was achieved by using **TFT1** as the emitting material. The convenient synthesis and multifunctional applications of the star-shaped oligomers claimed a novel series of useful optoelectronic materials.

Acknowledgment. Financial support from the Natural Science Foundation of China (NSFC, Nos. 20872171 and 60978055) is gratefully acknowledged.

Supporting Information Available: Spectroscopic analytical data for all new compounds and extra CV and TPEF spectra. This material is available free of charge via the Internet at http://pubs.acs.org.

References and Notes

(1) (a) Tang, C. W.; Van Slyke, S. A. *Appl. Phys. Lett.* **1987**, *51*, 913. (b) Friend, R. H.; Gymer, R. W.; Holmes, A. B.; Burroughes, J. H.; Marks, R. N.; Taliani, C.; Bradley, D. D. C.; Dos Santos, D. A.; Brédas, J. L.; Lögdlund, M.; Salaneck, W. R. *Nature* **1999**, *397*, 121. (c) Kraft, A.; Grimsdale, A. C.; Holmes, A. B. *Angew. Chem., Int. Ed. Engl.* **1998**, *37*, 402. (d) Grimsdale, A. C.; Chan, K. L.; Martin, R. E.; Jokisz, P. G.; Holmes, A. B. *Chem. Rev.* **2009**, *109*, 897.

(2) (a) Sariciftci, N. S.; Smilowitz, L.; Heeger, A. J.; Wudl, F. *Science* **1992**, *258*, 1474. (b) Halls, J. J. M.; Walsh, C. A.; Greenham, N. C.; Marseglia, E. A.; Friend, R. H.; Moratti, S. C.; Holmes, A. B. *Nature* **1995**, *376*, 498. (c) Huynh, W. U.; Dittmer, J. J.; Alivisatos, A. P. *Science* **2002**, *295*, 2425. (d) O'Regan, B.; Grätzel, M. *Nature* **1991**, *353*, 737. (e) Gunes, S.; Neugebauer, H.; Sariciftci, N. S. *Chem. Rev.* **2007**, *107*, 1324. (f) Coakley, K. M.; McGehee, M. D. *Chem. Mater.* **2004**, *16*, 4533.

(3) (a) Garnier, F.; Hajlaoui, R.; Yassar, A.; Shirakawa, P. *Science* **1994**, *265*, 1684. (b) Dimitrakopoulos, C. D.; Malenfant, P. R. L. *Adv. Mater.* **2002**, *14*, 99. (c) Sirringhaus, H. *Adv. Mater.* **2005**, *17*, 2411. (d) Muccini, M. *Nat. Mater.* **2006**, *5*, 605. (e) Murphy, A. R.; Fréchet, J. M. J. *Chem. Rev.* **2007**, *107*, 1066. (f) Braga, D.; Horowitz, G. *Adv. Mater.* **2009**, *21*, 1473. (g) Piliego, C.; Jarzab, D.; Gigli, G.; Chen, Z.; Facchetti, A.; Loi, M. A. *Adv. Mater.* **2009**, *21*, 1573.

(4) (a) Chen, C. T. *Chem. Mater.* **2004**, *16*, 4389. (b) Shah, B. K.; Neckers, D. C.; Shi, J. M.; Forsythe, E. W.; Morton, D. *Chem. Mater.* **2006**, *18*, 603. (c) Cheng, J.-A.; Chen, C. H.; Liao, C. H. *Chem. Mater.* **2004**, *16*, 2862. (d) Mitschke, U.; Bauerle, P. *J. Mater. Chem.* **2000**, *10*, 1471. (e) Jia, W. L.; Feng, X. D.; Bai, D. R.; Lu, Z. H.; Wang, S.; Vamvounis, G. *Chem. Mater.* **2005**, *17*, 164. (f) Roncali, J. *Acc. Chem. Res.* **2009**, *42*, 1719.

(5) (a) Burroughes, J. H.; Bradley, D. D. C.; Brown, A. R.; Marks, R. N.; MacKay, K.; Friend, R. H.; Burn, P. L; Holmes, A. B. *Nature* **1990**, *347*, 539. (b) Bernius, M. T.; Inbasekaran, M.; O'Brien, J.; Wu, W. *Adv. Mater.* **2002**, *14*, 1737. (c) Shim, H.; Jin, J. *Adv. Polym. Sci.* **2002**, *158*, 193. (d) Kulkarni, A. P.; Tonzola, C. J.; Babel, A.; Jenekhe, S. A. *Chem. Mater.* **2004**, *16*, 4556. (e) Yan, H.; Chen, Z.; Zheng, Y.; Newman, C.; Quinn, J. R.; Dötz, F.; Kastler, M.; Facchetti, A. *Nature* **2009**, *457*, 679.

(6) (a) Lo, S.-C.; Burn, P. L. *Chem. Rev.* **2007**, *107*, 1097. (b) Lee, T.; Landis, C. A.; Dhar, B. M.; Jung, B. J.; Sun, J.; Sarjeant, A.; Lee, H.-J.; Katz, H. E. *J. Am. Chem. Soc.* **2009**, *131*, 1692. (c) Geng, Y.; Culligan, S. W.; Trajkovska, A.; Wallace, J. U.; Chen, S. H. *Chem. Mater.* **2003**, *15*, 542. (d) Okumoto, K.; Shirota, Y. *Chem. Mater.* **2003**, *15*, 699. (e) Geng, Y.; Chen, A. C. A.; Ou, J. J.; Chen, S. H.; Klubek, K.; Vaeth, K. M.; Tang, C. W. *Chem. Mater.* **2003**, *15*, 4352. (f) Tonzola, C. J.; Kulkarni, A. P.; Gifford, A. P.; Kaminsky, W.; Jenekhe, S. A. *Adv. Funct. Mater.* **2007**, *17*, 863.

(7) (a) Pei, J.; Wang, J. L.; Cao, X. Y.; Zhou, X. H.; Zhang, W. B. *J. Am. Chem. Soc.* **2003**, *125*, 9944. (b) Zhou, X. H.; Yan, J. C.; Pei, J. *Org. Lett.* **2003**, *5*, 3543. (c) Kanibolotsky, A. L.; Berridge, R.; Skabara, P; J.; Perepichka, I. F.; Bradley, D. D. C.; Koeberg, M. *J. Am. Chem. Soc.* **2004**, *126*, 13695. (d) Cremer, J.; Baüerle, P. *J. Mater. Chem.* **2006**, *16*, 874. (e) Li, B.; Li, J.; Fu, Y.; Bo, Z. *J. Am. Chem. Soc.* **2004**, *126*, 3430.

(8) (a) Shirota, Y.; Kinoshita, M.; Noda, T.; Okumoto, K.; Ohara, T. *J. Am. Chem. Soc.* **2000**, *122*, 11021. (b) Doi, H.; Kinoshita, M.; Okumoto, K.; Shirota, Y. *Chem. Mater.* **2003**, *15*, 1080. (c) Thomas, K. R. J.; Velusamy, M.; Lin, J. T.; Chuen, C.-H.; Tao, Y.-T. *Chem. Mater.* **2005**, *17*, 1860. (d) Chen, S.; Xu, X.; Liu, Y.; Yu, G.; Sun, X.; Qiu, W.; Ma, Y.; Zhu, D *Adv. Funct. Mater.* **2005**, *15*, 1541. (e) Hancock, J. M.; Gifford, A. P.; Zhu, Y.; Lou, Y.; Jenekhe, S. A. *Chem. Mater.* **2006**, *18*, 4924. (f) Kulkarni, A. P.; Kong, X.; Jenekhe, S. A. *Adv. Funct. Mater.* **2006**, *16*, 1057. (g) Wang, J.; Tang, Z.; Xiao, Q.; Ma, Y.; Pei, J. *Org. Lett.* **2009**, *11*, 863.

(9) (a) Kato, S.; Matsumoto, T.; Shigeiwa, M.; Gorohmaru, H.; Maeda, S.; Ishi-i, T.; Mataka, S. *Chem.—Eur. J.* **2006**, *12*, 2303. (b) Kannan, R.; Reinhardt, B. A.; Tan, L.-S. U.S. Patent 6,300,502, Oct 9, 2001. (c) Kirkpatrick, S. M.; Baur, J. W.; Clark, C. M.; Denny, L. R.; Tomlin, D. W.; Reinhardt, B. R.; Kannan, R.; Stone, M. O. *Appl. Phys. A: Mater. Sci. Process.* **1999**, 69. (d) Liu, S.; Lin, K. S.; Churikov, V. M.; Su, Y. Z.; Lin, J. T.; Huang, T.-H.; Hsu, C. C. *Chem. Phys. Lett.* **2004**, *390*, 433.

(10) (a) Fang, T.; Shimp, D. A. *Prog. Polym. Sci.* **1995**, *20*, 61. (b) Kucharski, M.; Mazurkiewicz, W. *Polymer* **1982**, *23*, 1868. (c) Nishikubo, T.; Kameyama, A.; Saito, C. *J. Polym. Sci., Polym. Chem.* **2000**, *38*, 3604.

(11) (a) Nenner, I.; Schulz, G. J. *J. Chem. Phys.* **1975**, *62*, 1747. (b) Fink, R.; Frenz, C.; Thelakkat, M.; Schmidt, H. *Macromolecules* **1997**, *30*, 8177. (c) Fink, R.; Heischkel, Y.; Thelakkat, M.; Schmidt, H. *Chem. Mater.* **1998**, *10*, 3620. (d) Meier, H.; Holst, H. C.; Oehlhof, A. *Eur. J. Org. Chem.* **2003**, 4173. (e) Meier, H.; Karpuk, E.; Holst, H. C. *Eur. J. Org. Chem.* **2006**, 2609. (f) Fang, Q.; Ren, S.; Xu, B.; Du, J.; Cao, A. *J. Polym. Sci., Polym. Chem.* **2006**, *44*, 3797. (g) Yamamoto, T.; Watanabe, S.; Fukumoto, H.; Sato, M.; Tanaka, T. *Macromol. Rapid Commun.* **2006**, *27*, 317. (h) Zou, L.; Fu, Y.; Yan, X.; Chen, X.; Qin, J. *J. Polym. Sci., Polym. Chem.* **2008**, *46*, 702.

(12) (a) Kang, J.; Lee, D.; Park, H.; Park, Y.; Kim, J. W.; Jeong, W.; Yoo, K.; Go, K.; Kim, S.; Kim, J. *J. Mater. Chem.* **2007**, *17*, 3714. (b) Richard, A.; Klenklera, H. A.; Tranc, A.; Popovic, D. Z.; Xu, G. *Org. Electron.* **2008**, *9*, 285. (c) Zhong, H.; Xu, E.; Zeng, D.; Du, J.; Sun, J.; Ren, S.; Jiang, B.; Fang, Q. *Org. Lett.* **2008**, *10*, 709.

(13) (a) Pang, J.; Tao, Y.; Freiberg, S.; Yang, X.-P.; D'; Iorio, M.; Wang, S. *J. Mater. Chem.* **2002**, *12*, 206. (b) Kim, S. W.; Shim, S. C.; Jung, B.-J.; Shim, H.-K. *Polymer* **2002**, *43*, 4297. (c) Jia, W.; Hu, Y.; Gao, J.; Wang, S. *Dalton Trans.* **2006**, 1721. (d) Wen, G.; Xin, Y.; Zhu, X.; Zeng, W.; Zhu, R.; Feng, J.; Cao, Y.; Zhao, L.; Wang, L.; Wei, W.; Peng, B.; Huang, W. *Polymer* **2007**, *48*, 1824.

(14) (a) Inomata, H.; Goushi, K.; Masuko, T.; Konno, T.; Imai, T.; Sasabe, H.; Brown, J. J.; Adachi, C. *Chem. Mater.* **2004**, *16*, 1285. (b) Son, K.; Yahiro, M.; Imai, T.; Yoshizaki, H.; Adachi, C. *Chem. Mater.* **2008**, *20*, 4439. (c) Haneder, S.; Da Como, E.; Feldmann, J.; Rothmann, M. M.; Strohriegl, P.; Lennartz, C.; Molt, O.; Münster, I.; Schildknecht, C.; Wagenblast, G. *Adv. Funct. Mater.* **2009**, *19*, 2416. (d) Rothmann, M. M.; Haneder, S.; Da Como, E.; Lennartz, C.; Schildknecht, C.; Strohriegl, P. *Chem. Mater.* **2010**, *22*, 2403.

(15) Kannan, R.; He, G. S.; Lin, T.-C.; Prasad, P. N.; Vaia, R. A.; Tan, L.-S. *Chem. Mater.* **2004**, *16*, 185.

(16) Zou, L.; Liu, Z.; Yan, X.; Liu, Y.; Fu, Y.; Liu, J.; Huang, Z.; Chen, X.; Qin, J. *Eur. J. Org. Chem.* **2009**, 5587.

(17) (a) Murase, T.; Fujita, M. *J. Org. Chem.* **2005**, *70*, 9269. (b) Kim, C. K.; Song, E. S.; Kim, H. J.; Park, C.; Kim, Y. C.; Kim, J. K.; Yu, J. W.; Kim, C. *J. Polym. Sci., Polym. Chem.* **2006**, *44*, 254. (c) Leriche, P.; Piron, F.; Ripaud, E.; Frère, P.; Allain, M.; Roncali, J. *Tetrahedron Lett.* **2009**, *50*, 5673.

(18) Ding, J.; Day, M.; Robertson, G.; Roovers, J. *Macromolecules* **2002**, *35*, 3474.

(19) McIlroy, S. P.; E., Cló; Nikolajsen, L.; Frederiksen, P. K.; Nielsen, C. B.; Mikkelsen, K. V.; Gothelf, K. V.; Ogilby, P. R. *J. Org. Chem.* **2005**, *70*, 1134.

(20) Kulkarni, A. P.; Zhu, Y.; Babel, A.; Wu, P.-T.; Jenekhe, S. A. *Chem. Mater.* **2008**, *20*, 4212.

(21) Mani, S. E.; Jang, J. I.; Ketterson, J. B. *Opt. Lett.* **2009**, *34*, 2817.

(22) Jang, J. I.; Mani, S.; Ketterson, J. B.; Lovera, P.; Redmond, G. *Appl. Phys. Lett.* **2009**, *95*, 221906.

JP104710Y